Local skin friction and heat transfer in combined free-forced convection from a cylinder or sphere to a power-law fluid

T.-Y. Wang and C. Kleinstreuer*
Department of Mechanical and Aerospace Engineering, North Carolina State University, Raleigh, NC 27695-7910, USA

Received 11 June 1987 and accepted for publication 18 August 1987

Steady-state laminar heat transfer mechanisms of polymeric liquids flowing across a horizontal cylinder or past a sphere of different wall temperatures have been analyzed. The uniquely transformed conservation equations of this nonsimilar problem have been solved with an implicit finite difference method up to the point of boundary layer separation. Of interest are the effects of the power-law index, the buoyancy parameter, and a generalized Prandtl number on the local skin friction coefficient and the local Nusselt number. Both the dimensionless skin friction group and the heat transfer group increase with higher buoyancy effects for any power-law fluid. Furthermore, increasing the buoyancy force will delay the point of flow separation. Dilatant fluids exhibit a distinctively different heat transfer behavior than pseudoplastics in the vicinity of the stagnation point. Higher Prandtl numbers generate lower skin friction and larger heat transfer coefficients.

Keywords: skin friction/heat transfer group; combined free-forced convection, non-Newtonian fluid; horizontal cylinder/sphere; heating/cooling

Introduction

Of basic interest in fluid mechanics and heat transfer are steady temperature and pressure-driven flows of non-Newtonian fluids across horizontal cylinders or spheres. Applications for such systems can be found in industries processing molten plastics, polymers, food stuff, or slurries. Thus considerable attention has been directed toward major aspects of this coupled, nonlinear boundary layer problem[1-5]. For example, Acrivos, Shah, and Peterson[2] analyzed forced convection heat transfer between a horizontal cylinder and a power-law fluid of infinitely large Prandtl numbers. Kim, Jeng, and DeWitt[3], as other researchers before them, employed a Merk series expansion to solve the forced convection problem for a horizontal cylinder and non-Newtonian fluids. Recently, Nakayama and Koyama[4] used the von Karman integral method to obtain an asymptotic solution for forced convection in high non-Newtonian Prandtl number fluids. The mixed thermal convection problem for a horizontal cylinder and for a sphere submerged in a Newtonian fluid has been solved by Mucoglu and Chen[5] and Chen and Mucoglu[6], respectively.

In this paper, combined free and forced convection from a horizontal cylinder or a sphere to power-law fluids has been investigated. Both heated and cooled isothermal surfaces have been considered to study the effects of aiding and opposing buoyancy flows in relation to the upward forced convection stream. The distributions of the dimensionless skin friction and heat transfer groupings are computed for the region of attached boundary layer flows. Empirical correlations have been used for the associated outer flow velocities. The coupled nonlinear partial differential equations for non-Newtonian fluid flow and combined heat transfer have been reduced with a powerful nonsimilar transformation and then solved using an implicit finite difference scheme. This approach to the problem solution is more accurate and more efficient than conventional methods such as power series expansions, weighted residual methods, or direct finite differencing.

* To whom all correspondence should be addressed.

Analysis

The system schematics and a suitable coordinate system are given in Figure 1. The distance $r(x)$ needed for the sphere is $r(x) = R \sin(x/R)$. The surface of the cylinder or sphere of radius R is maintained at a constant temperature T_w. The isothermal wall temperature may be above or below T_∞, depending upon the operational mode of heating ($Z = 1$) or cooling ($Z = -1$). The gravitational force is acting downward while the uniform forced flow (u_∞, T_∞) is moving upward. Natural convection will assist the forced boundary layer flow for heated surfaces ($T_w > T_\infty$) and will retard the forced flow in the cooled cylinder/sphere case, i.e., when $T_w < T_\infty$. The analysis is also valid for downward flow; however, the x-coordinate is then measured from the upper stagnation point.

Using the standard power-law viscosity model and the Boussinesq assumption, the boundary layer equations for steady laminar flow without wake effects and cylinder end effects are (Figure 1)

$$\frac{\partial(ru)}{\partial x} + \frac{\partial(rv)}{\partial y} = 0 \tag{1}$$

$$u\frac{\partial u}{\partial x} + v\frac{\partial u}{\partial y} = u_e\frac{du_e}{dx} + Zg\beta|T - T_\infty|\sin\frac{x}{R} + \frac{K}{\rho}\frac{\partial}{\partial y}\left(\left|\frac{\partial u}{\partial y}\right|^{n-1}\frac{\partial u}{\partial y}\right) \tag{2}$$

and

$$u\frac{\partial T}{\partial x} + v\frac{\partial T}{\partial y} = \alpha\frac{\partial^2 T}{\partial y^2} \tag{3}$$

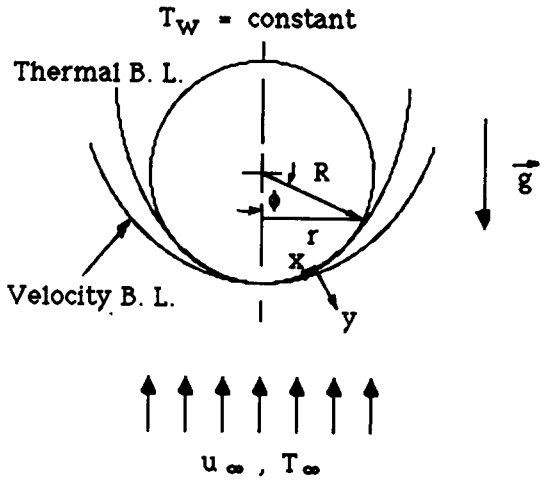

Figure 1 System schematics and coordinates

The associated boundary conditions are

$$u=v=0 \quad \text{and} \quad T=T_w \qquad \text{at } y=0 \tag{4a}$$

and

$$u=u_e(x) \quad \text{and} \quad T=T_\infty \qquad \text{at } y=\infty \tag{4b}$$

where

$$\frac{u_e}{u_\infty}=0.92\left(\frac{x}{R}\right)-0.131\left(\frac{x}{R}\right)^3 \tag{5}$$

for a cylinder in crossflows[8] and

$$\frac{u_e}{u_\infty}=1.5\left(\frac{x}{R}\right)-0.4371\left(\frac{x}{R}\right)^3+0.1481\left(\frac{x}{R}\right)^5-0.0423\left(\frac{x}{R}\right)^7 \tag{6}$$

for a sphere[9]. The empirical edge velocity distribution (6) has been measured with Newtonian fluids, whereas Equation 5 has been developed for both types of fluids. It is assumed that both equations hold for $0.5 \leqslant n \leqslant 1.6$.

With the stream-function approach

$$u=\frac{1}{r}\frac{\partial \psi}{\partial y} \tag{7a}$$

$$v=-\frac{1}{r}\frac{\partial \psi}{\partial x} \tag{7b}$$

and the transformations

$$\xi=\frac{x}{R} \tag{8a}$$

$$\eta=\left(\frac{\mathrm{Re}}{\xi}\right)^{1/(n+1)}\left(\frac{u_e}{u_\infty}\right)^{(2-n)/(n+1)}\frac{y}{R} \tag{8b}$$

$$\theta(\xi,\eta)=\frac{T-T_\infty}{T_w-T_\infty} \tag{8c}$$

$$\psi=rRu_\infty\left(\frac{\xi}{\mathrm{Re}}\right)^{1/(n+1)}\left(\frac{u_\infty}{u_e}\right)^{(1-2n)/(n+1)}F(\xi,\eta) \tag{8d}$$

the governing equations, Equations 1–3, are reduced to

$$(|F''|^{n-1}F'')'+\gamma(\xi)FF''+\Lambda(\xi)(1-F'^2) = -Z\theta\lambda\Omega(\xi)+\xi\left(F'\frac{\partial F'}{\partial \xi}-F''\frac{\partial F}{\partial \xi}\right) \tag{9}$$

$$\frac{E(\xi)}{\mathrm{Pr}}\theta''+\gamma(\xi)F\theta'=\xi\left(F'\frac{\partial \theta}{\partial \xi}-\theta'\frac{\partial F}{\partial \xi}\right) \tag{10}$$

The transformations are based on scale analysis and non-dimensionalization of the governing equations (cf. Ref. 10). The generalized Reynolds number is

$$\mathrm{Re}=\frac{\rho u_\infty^{2-n}R^n}{K} \tag{11a}$$

and the generalized Prandtl number is

$$\mathrm{Pr}=\frac{u_\infty R}{\alpha}\mathrm{Re}^{-2/(n+1)} \tag{11b}$$

The new coefficients in Equations 9 and 10 are defined as

$$\Lambda(\xi)=\frac{\xi}{u_e}\frac{\mathrm{d}u_e}{\mathrm{d}\xi} \tag{12a}$$

$$\gamma(\xi)=\frac{1}{n+1}+\left(\frac{2n-1}{n+1}\right)\Lambda(\xi)+\frac{\xi}{r}\frac{\mathrm{d}r}{\mathrm{d}\xi} \qquad \text{for the sphere} \tag{12b}$$

Notation

- c_f Local skin friction coefficient
- F Dimensionless stream function
- g Gravitational acceleration
- Gr Generalized Grashof number
- h Local heat transfer coefficient
- K Fluid consistency index for power-law fluid
- k Thermal conductivity
- Nu Local Nusselt number
- n Flow index for power-law fluid
- Pr Generalized Prandtl number
- Re Generalized Reynolds number
- R Radius of cylinder or sphere
- r Distance from axis of symmetry to body surface, $r=R\sin\phi$
- T Temperature
- u Velocity component in x-direction
- v Velocity component in y-direction
- x Streamwise coordinate measured along surface from forward stagnation point
- y Coordinate normal to surface
- Z Dimensionless parameter, $Z=1$ for heated and $Z=-1$ for cooled submerged body

Greek symbols

- α Thermal diffusivity
- β Thermal expansion coefficient
- η Dimensionless parameter
- λ Buoyancy parameter
- θ Dimensionless temperature
- ρ Density of fluid
- τ Shear stress
- ξ Dimensionless parameter, $\xi=x/R$
- ϕ Angular coordinate
- ψ Stream function

Subscripts

- e Boundary layer edge condition
- ∞ Ambient condition
- w Wall condition

Table 1 Data comparison of the skin friction group, $\frac{1}{2}c_f \mathrm{Re}^{1/(n+1)}$, for forced convection across a horizontal, heated cylinder

$\xi = \frac{x}{R}$	$n=0.52$		$n=1.6$	
	Kim *et al.*[3]	Present method	Kim *et al.*[3]	Present method
0.1	0.2445	0.2445	0.09869	0.09884
0.2	0.3902	0.3902	0.1360	0.1365
0.4	0.6095	0.6099	0.3030	0.3043
0.6	0.7659	0.7685	0.4561	0.4569
0.8	0.8661	0.8718	0.5680	0.5679
1.0	0.9015	0.9174	0.6169	0.6138
1.2	0.8859	0.8995	0.5825	0.5774
1.4	0.7901	0.8067	0.4571	0.4469
1.5	0.6791	0.7252	0.3462	0.3440

and

$$\gamma(\xi) = \frac{1}{n+1} + \left(\frac{2n-1}{n+1}\right)\Lambda(\xi) \qquad \text{for the cylinder} \quad (12c)$$

$$\Omega(\xi) = \frac{\xi \sin \xi}{(u_e/u_\infty)^2} \qquad (12d)$$

$$E(\xi) = (u_e/u_\infty)^{3(1-n)/(n+1)} \xi^{(n-1)/(n+1)} \qquad (12e)$$

and the buoyancy parameter is

$$\lambda = \frac{\mathrm{Gr}}{\mathrm{Re}^{2/(2-n)}} \qquad (13a)$$

where

$$\mathrm{Gr} = (K/\rho)^{2/(n-2)} g\beta(T_w - T_\infty) R^{(2+n)/(2-n)} \qquad (13b)$$

is the generalized Grashof number.

The transformed boundary conditions (4a) and (4b) read

$$\text{at } \eta = 0: \quad F'(\xi,0) = 0, \quad \gamma(\xi)F(\xi,0) + \xi \left.\frac{\partial F}{\partial \xi}\right|_{\eta=0} = 0$$

$$\text{and} \quad \theta(\xi,0) = 1 \qquad (14a)$$

$$\text{at } \eta = \infty: \quad F'(\xi,\infty) = 1 \quad \text{and} \quad \theta(\xi,\infty) = 0 \qquad (14b)$$

With the definition of the local skin friction coefficient, $c_f = 2\tau_w/\rho u_\infty^2$, a dimensionless skin friction group (SFG) can be formed as

$$\tfrac{1}{2}c_f \mathrm{Re}^{1/(n+1)} = \xi^{-n/(n+1)} \left(\frac{u_e}{u_\infty}\right)^{3n/(n+1)} [F''(\xi,0)]^n \qquad (15)$$

Similarly, with the definition of the local Nusselt number, $\mathrm{Nu} = hR/k$, a heat transfer group (HTG) is formed as

$$\mathrm{Nu}\,\mathrm{Re}^{-1/(n+1)} = -\xi^{-1/(n+1)} \left(\frac{u_e}{u_\infty}\right)^{(2-n)/(n+1)} \theta'(\xi,0) \qquad (6)$$

Numerical solution method

The system of coupled nonlinear equations (9) and (10) subject to the boundary edge and boundary conditions (5) or (6) and (14a), (14b), respectively, are solved using Keller's box method outlined in Cebeci and Bradshaw[11]. The governing equations are first written in the form of a first-order system by introducing new unknown functions of η-derivatives. The functions and their derivatives in the first-order differential equations are then approximated by centered difference quotients and averaged at the midpoints of grid rectangles in the (ξ,η)-domain or the segments in the ξ and η coordinates, as required. The resulting nonlinear difference equations together with the finite difference approximation of the boundary conditions are solved iteratively using Newton's linearization method. The accuracy is of the order of $(\Delta\xi)^2$ or $(\Delta\eta)^2$, which can be improved to fourth-order accuracy using Richardson extrapolation. A two-dimensionally nonuniform mesh is required, which is extremely fine in the vicinity of the stagnation point and very fine near the separation point, the body surface, and the boundary layer edge. Although Keller's box method is a parabolic code, it accurately predicts the angle of boundary layer separation as previously tested under more severe flow conditions[12].

Results and discussion

The lack of experimental data sets for the present system required comparisons of our reduced computer simulation model with special case studies found in the open literature. Table 1 lists values of the predicted SFG and results obtained by Kim, Jeng, and DeWitt[3] for forced convection heat transfer of a non-Newtonian fluid ($n=0.52$ and 1.6) across a horizontal cylinder. The agreement is very good in the front region of the cylinder, i.e., when $x/R < 1.0$. However, for larger x/R values the results of the Merk series expansion[3] become somewhat erroneous, especially for pseudoplastics ($n < 1.0$). In a separate simulation study we reproduced exactly the same graphs as found in the literature showing SFG and HTG profiles for combined free-forced convection heat transfer of a Newtonian fluid across a horizontal cylinder[5] and about a sphere[6].

Of interest in this paper are the angular distributions of Equation 15, $\mathrm{SFG} \equiv \frac{1}{2}c_f \mathrm{Re}^{1/(n+1)}$, and Equation 16, $\mathrm{HTG} \equiv \mathrm{Nu}/\mathrm{Re}^{1/(n+1)}$, for mixed thermal convection of power-law fluids. Their effects with the buoyancy force as a parameter are shown in Figures 2–5. Figure 2 depicts the variation of SFG along the heated cylinder surface for a generalized Prandtl number of $\mathrm{Pr} = 100$. Clearly, pseudoplastics generate higher and dilatant fluids lower wall shear stresses than Newtonian fluids. Natural convection aiding the forced flow increases SFG and helps to delay boundary layer separation (SFG = 0). Figure 3 indicates that both the power-law index n and the buoyancy parameter λ are less influential on the SFG distribution for spheres than for horizontal cylinders (Figure 2). Figures 4 and 5 show the local

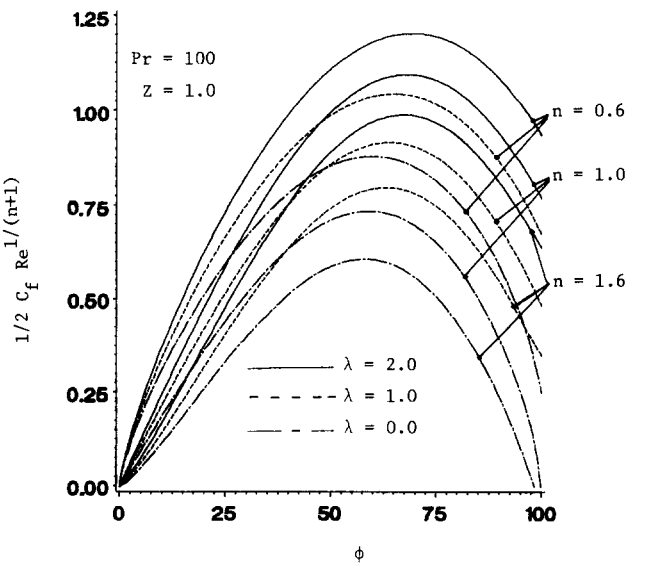

Figure 2 Angular distribution of SFG for a heated cylinder

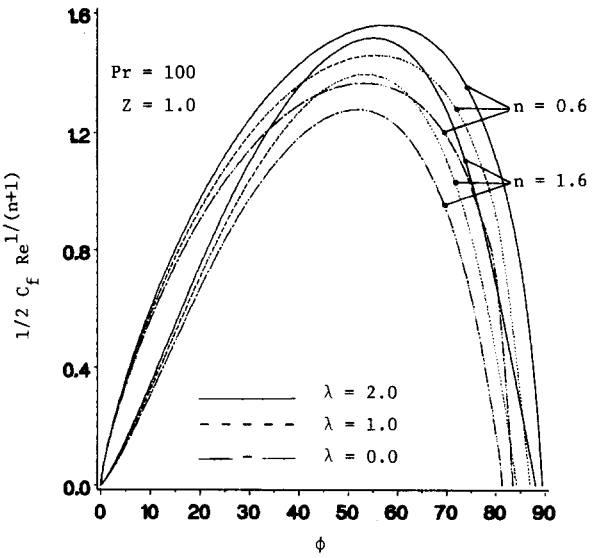

Figure 3 Angular distribution of SFG for a heated sphere

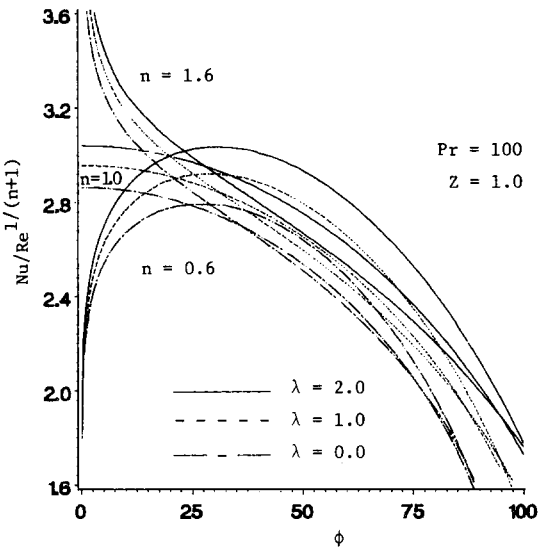

Figure 4 Angular distribution of HTG for a heated cylinder

HTG for heated cylinders and spheres, respectively. For Newtonian fluids ($n = 1.0$), the local generalized Nusselt number decreases monotonously along the curved surfaces. The unique thermal behavior of non-Newtonian fluids ($n \neq 1.0$) near the stagnation point is similar to that for the vertical cylinder configuration[10]. Pseudoplastics ($n < 1.0$) reach rapidly a maximum in HTG(ϕ), and then, similar to Newtonian fluids, the HTG decreases gradually. In contrast, the HTG for dilatant fluids reduces very rapidly in the vicinity of $\xi = 0$ and then follows, after a point of inflection, the general trend of HTG(ϕ) for Newtonian fluids. The significantly different behavior of the two types of power-law fluids near the stagnation point can be explained as follows. As can be deduced from Equation 16,

$$\mathrm{HTG} \sim \xi^{(1-n)/(n+1)}, \qquad \theta'(\xi, 0)$$

which implies that for $\xi \to 0$

$$\mathrm{HTG} \to \begin{cases} 0 & \text{for } n < 1.0 \\ \infty & \text{for } n > 1.0 \end{cases}$$

provided that θ' is well behaved at the stagnation point. The thermal behavior of all fluids is quite similar for both bodies, although the influence of λ is again larger for horizontal cylinders.

An increase in Pr decreases the SFG and increases the HTG distributions for any fluid (cf. Figures 6(a), (b) and 7(a), (b)). Higher values of $\mathrm{Pr} \propto K/\alpha$ imply more viscous fluids, which reduces SFG $\propto 1/K$. The opposite effect can be observed for the HTG profiles that shift upward with higher Prandtl numbers, because $\mathrm{Pr} \propto 1/\alpha$ and fluids with smaller thermal diffusivities generate higher dimensionless temperature gradients at the wall.

In various industrial applications the wall temperature is lower than the free-stream temperature, and hence it is of interest to analyze the effect of cooled cylinders or spheres on the SFG and HTG profiles (cf. Figures 8(a), (b) and 9(a), (b)). Submerged bodies with $T_w < T_\infty$ have lower SFG and HTG values. The trend is quite comparable to the effect of lowering

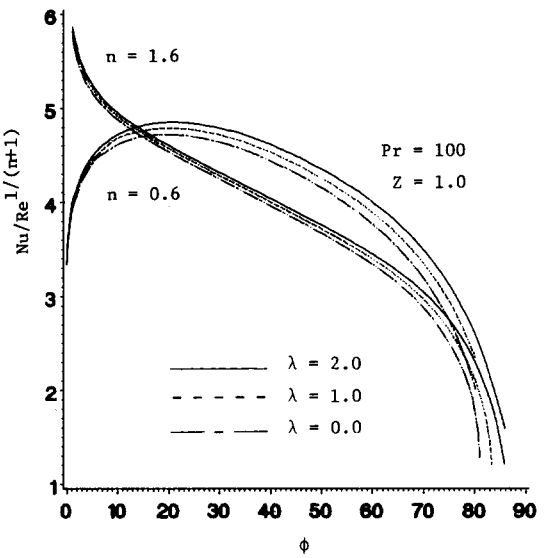

Figure 5 Angular distribution of HTG for a heated sphere

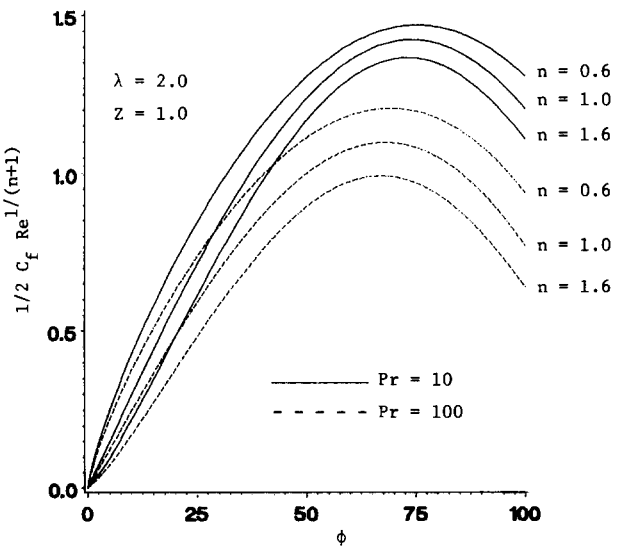

Figure 6(a) The effects of the generalized Prandtl number on SFG for a heated cylinder

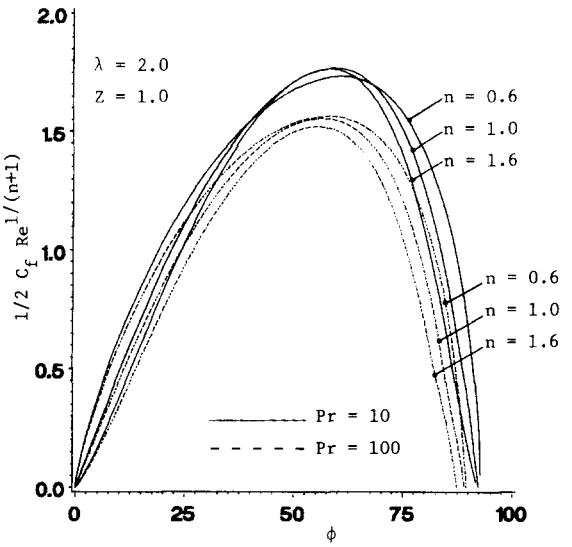

Figure 6(b) The effects of the generalized Prandtl number on SFG for a heated sphere

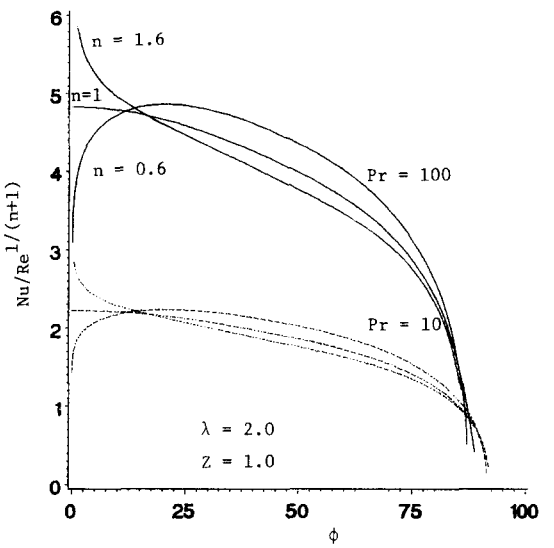

Figure 7(b) The effects of the generalized Prandtl number on HTG for a heated sphere

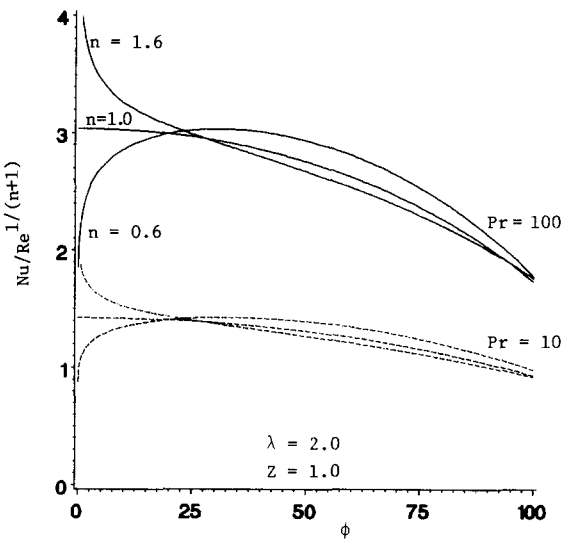

Figure 7(a) The effects of the generalized Prandtl number on HTG for a heated cylinder

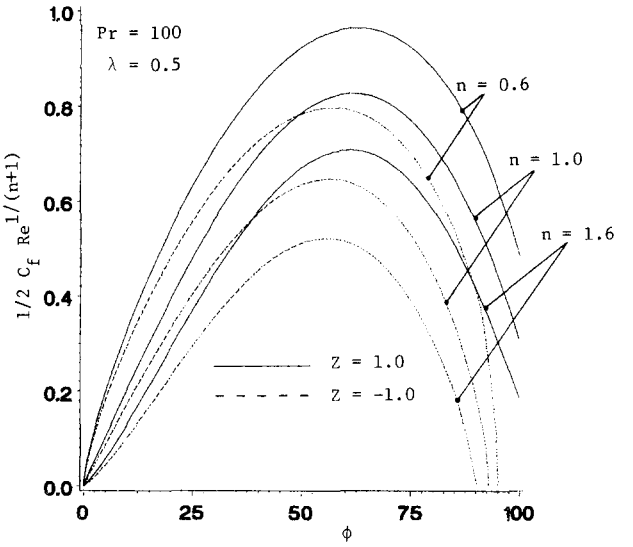

Figure 8(a) Comparison of SFG for heated and cooled cylinder

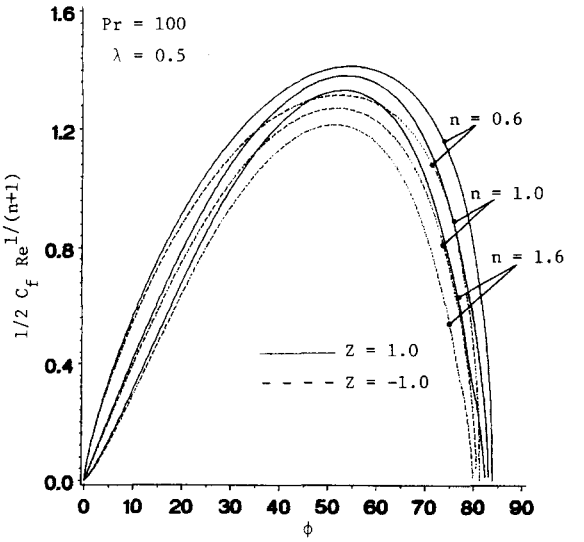

Figure 8(b) Comparison of SFG for heated and cooled sphere

the buoyancy parameter (cf. Figures 2–5). In these cases, forced convection is either retarded by the opposing buoyancy force (cooled cylinder/sphere) or relatively less enhanced by decreasing the buoyancy force (reduction of λ). As can be expected, the separation angle for opposing flow ($Z = -1$ in Figures 8(a) and 8(b)) is smaller than that of aiding flow ($Z = 1.0$).

Conclusions

Two important wall variables, the local SFG and the local HTG, have been analyzed for mixed thermal convection of a power-law fluid flowing upward past a horizontal cylinder or sphere. The isothermal, submerged bodies are either heated where natural convection assists the forced flow or cooled where buoyancy retards the forced momentum transfer. In addition to the influence of heating ($Z = 1$) versus cooling ($Z = -1$), the

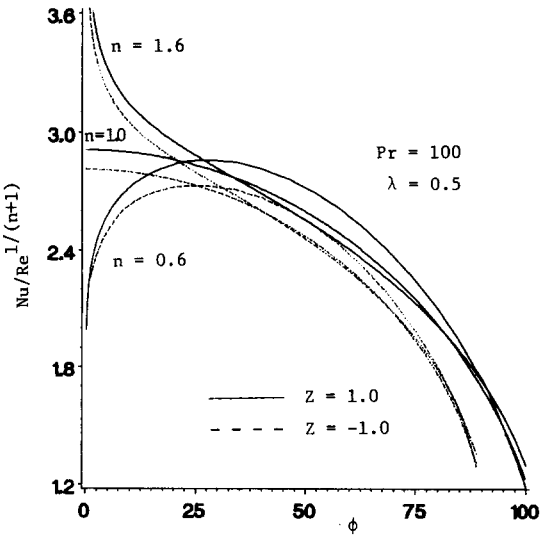

Figure 9(a) Comparison of HTG for heated and cooled cylinder

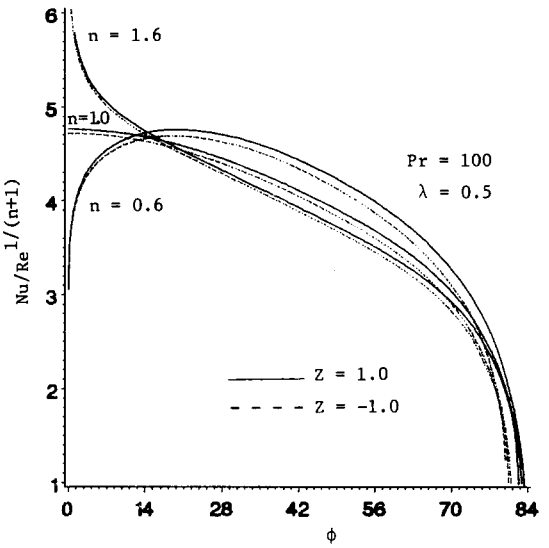

Figure 9(b) Comparison of HTG for heated and cooled sphere

effects of n, Pr, and λ on SFG and HTG have been studied for both horizontal cylinders and spheres.

In general, changes in all system parameters; i.e., Z, n, Pr, and/or λ, have a more pronounced effect on SFG and HTG for horizontal cylinders than for spheres. The angular distribution of HTG for power-law fluids near the stagnation point is distinctively different from the heat transfer behavior of Newtonian fluids. Pseudoplastics exhibit a maximum for HTG(ϕ), whereas the local HTG for dilatant fluids reduces sharply near $\xi=0$ and then follows the behavior of HTG for Newtonian fluids. As expected, a cooled surface, like a decrease in λ, reduces the angle of boundary layer separation. Higher-Prandtl-number fluids decrease SFG values and increase the local heat transfer coefficient.

References

1 Shenoy, A. V. and Mashelkar, R. A. Thermal convection in non-Newtonian fluids. *Adv. Heat Transfer*, 1982, **15**, 143–225

2 Acrivos, A., Shah, M. J., and Peterson, E. E. On the solution of the two-dimension boundary-layer flow equations for a non-Newtonian power law fluid. *Chem. Engng. Sci.*, 1965, **20**, 101–105

3 Kim, H. W., Jeng, D. R., and DeWitt, K. J. Momentum and heat transfer in power-law fluid flow over two-dimensional or axisymmetrical bodies. *Int. J. Heat Mass Transfer*, 1983, **26**, 245–259

4 Nakayama, A. and Koyama, H. An asymptotic expression for forced convection in non-Newtonian power-law fluids. *Int. J. Heat Fluid Flow*, 1986, **3**, 99–101

5 Mucoglu, A. and Chen, T. S. Analysis of combined forced and free convection across a horizontal cylinder. *Can. J. Chem. Eng.*, 1977, **55**, 265–271

6 Chen, T. S. and Mucoglu, A. Analysis of mixed forced and free convection about a sphere. *Int. J. Heat Transfer*, 1977, **20**, 867–875

7 Bird, R. B., Armstrong, R. C., and Hassager, O. *Dynamics of Polymeric Liquids*, Vol. 1, Wiley, New York, 1979

8 Shah, M. J., Peterson, E. E., and Acrivos, A. Heat transfer from a cylinder to a power-law non-Newtonian fluid. *AIChE J.*, 1962, **8**, 542–549

9 Fage, A. In: *Viscous Fluid Flow*, F. M. White. McGraw-Hill, New York, 1974

10 Wang, T.-Y. and Kleinstreuer, C. Combined free-forced convection heat transfer between vertical slender cylinders and power-law fluids. *Int. J. Heat Mass Transfer*, 1988, **31**, 91–98

11 Cebeci, T. and Bradshaw, P. *Momentum Transfer in Boundary Layers*, Hemisphere, Washington, D.C., 1977

12 Kleinstreuer, C. and Eghlima, A. Analysis and simulation of new approximation equations for boundary-layer flow on curved surfaces. *Math. & Comp. in Simul.*, 1985, **27**, 307–325